Astron. Astrophys. 315, L229–L232 (1996)

ASTRONOMY AND ASTROPHYSICS

The ISO-SWS spectrum of P Cygni*

H.J.G.L.M. Lamers[1,2]**, F. Najarro**[3]**, R.P.Kudritzki**[3,4]**, P.W. Morris**[5,2]**, R.H.M. Voors**[1,2]**, J.I. van Gent**[1,2]**, L.B.F.M. Waters**[6,7]**, Th. de Graauw**[7]**, D. Beintema**[5,7]**, E.A. Valentijn**[5,7]**, and D.J. Hillier**[8]

[1] Astronomical Institute, University of Utrecht, Princetonplein 5, 3584 CC Utrecht, The Netherlands
[2] SRON Laboratory for Space Research, Sorbonnelaan 2, 3584 CA Utrecht, The Netherlands
[3] Institut für Astronomie und Astrophysik der Universität München, Scheinerstr. 1, D-81679 München, Germany
[4] Max-Planck-Institut für Astrophysik, Karl-Schwarzschild-Str. 1, D-85740 Garching bei München, Germany
[5] ISO Science Operations Center, Astrophysics Division of ESA, PO Box 50727, E-28080 Villafranca, Madrid, Spain
[6] Astronomical Institute Anton Pannekoek, University of Amsterdam, Kruislaan 403, 1098 SJ Amsterdan, The Netherlands
[7] SRON Laboratory for Space Research, PO Box 800, 9700 AV Groningen, The Netherlands
[8] Department of Physics and Astronomy, University of Pittsburgh, 3941 O'Hara Street, Pittsburgh, PA 15260, USA

Received 23 July 1996 / Accepted 13 August 1996

Abstract. The free-free IR excess and the IR emission lines of H and He I of the Luminous Blue Variable P Cygni are observed with the $ISO-SWS$ instrument. The observed profiles and the free-free emission are compared with predictions from a non-LTE model atmosphere with a stellar wind. The observations agree very well with a model that has the following properties: $T_{\rm eff}$ = 18100 K, R_* = 76 $R_\odot$, He/H=0.30 by number, $\dot{M}$ = 3.0 × 10^{-5} $M_\odot\,{\rm yr}^{-1}$ and v_∞=185 km s^{-1}. We observed forbidden emission lines of [Fe II], [Fe III], [Ni II], [Ne II], [Ne III] and [Si II]. ¿From the study of the [Ne II] and [Ne III] lines we find that the Ne abundance is about three times higher than normal. This may be due to clumping in the CS envelope at $r \simeq 10^3\ R_*$.

Key words: stars: early-type – stars: mass-loss – stars: atmospheres – stars: supergiants – stars: individual: P Cygni

1. Introduction

After two major outbursts in 1600 and 1660 followed by three decades of irregular photometric variations, the Luminous Blue Variable (LBV) star P Cygni (HD 193237) entered around 1700 into a relatively quiet phase. The star shows small irregular photometric variations of only about 0.2 magn., which is much smaller than the variations of up to 2 magn. observed for other LBVs (see reviews by Humphreys & Davidson 1994 and Lamers 1996).

Lamers and de Groot (1992) showed on the basis of historic observations that P Cygni is slowly evolving to the right in the HR-diagram. This suggests that the star has evolved off the main sequence and is now going through a phase of high mass loss with occasional eruptions. Langer et al. (1994) reached a similar conclusion based on new evolutionary calculations with very high mass loss and placed the star at the end of the hydrogen shell burning phase.

To gain further insight into the nature and the evolutionary phase of P Cygni we observed the star with the ISO *Short Wavelength Spectrometer*. The line profiles provide sensitive diagnostics of the transition region between the photosphere and the wind. We also study the forbidden lines of Ne^{+} and Ne^{++} which are formed in the circumstellar (CS) envelope.

2. Observations and data reduction

The IR energy distribution of P Cygni between 2.38 and 45.2 μm was measured with the $ISO-SWS$ instrument (Kessler et al. 1996; de Graauw et al. 1996) with the ISO Astronomical Observing Template (AOT) S01 on JD 50071.295. The integration time is 31 minutes and the nominal (point source) resolution is $\lambda/\Delta\lambda \simeq 250 - 600$. The star was also observed with SWS using AOT S06 on JD 50172.594 over 21 separate wavelength intervals. This required an integration time of $\simeq$ 2.5 hrs for a requested S/N ratio of 30. The intervals were selected on the positions of the H and He lines, plus several expected forbidden fine structure lines of interest. The spectral resolution in the intervals ranges from $\simeq$ 1000 to 2600, depending on the aperture, spectral order and detector block (cf de Graauw et al. 1996). The data reduction was performed consistently with the procedures used for the S01 Observations of LBVs of Lamers, Morris et al. (1996). We refer the reader to Schaeidt et al. (1996) and Valentijn et al. (1996) for a description of the instrument, the reduction software and the calibrations.

3. The emission lines of H and He I

3.1. The model

For the spectroscopic analysis of the IR spectrum of P Cyg we proceed as described by Najarro et al. (1994) and use the itera-

Send offprint requests to: H.J.G.L.M. Lamers

* Based on observations made with ISO, an ESA project with instuments funded by the ESA member states (especially the PI countries: France, Germany, the Netherlands and the United Kingdom) with the participation of $ISAS$ and $NASA$

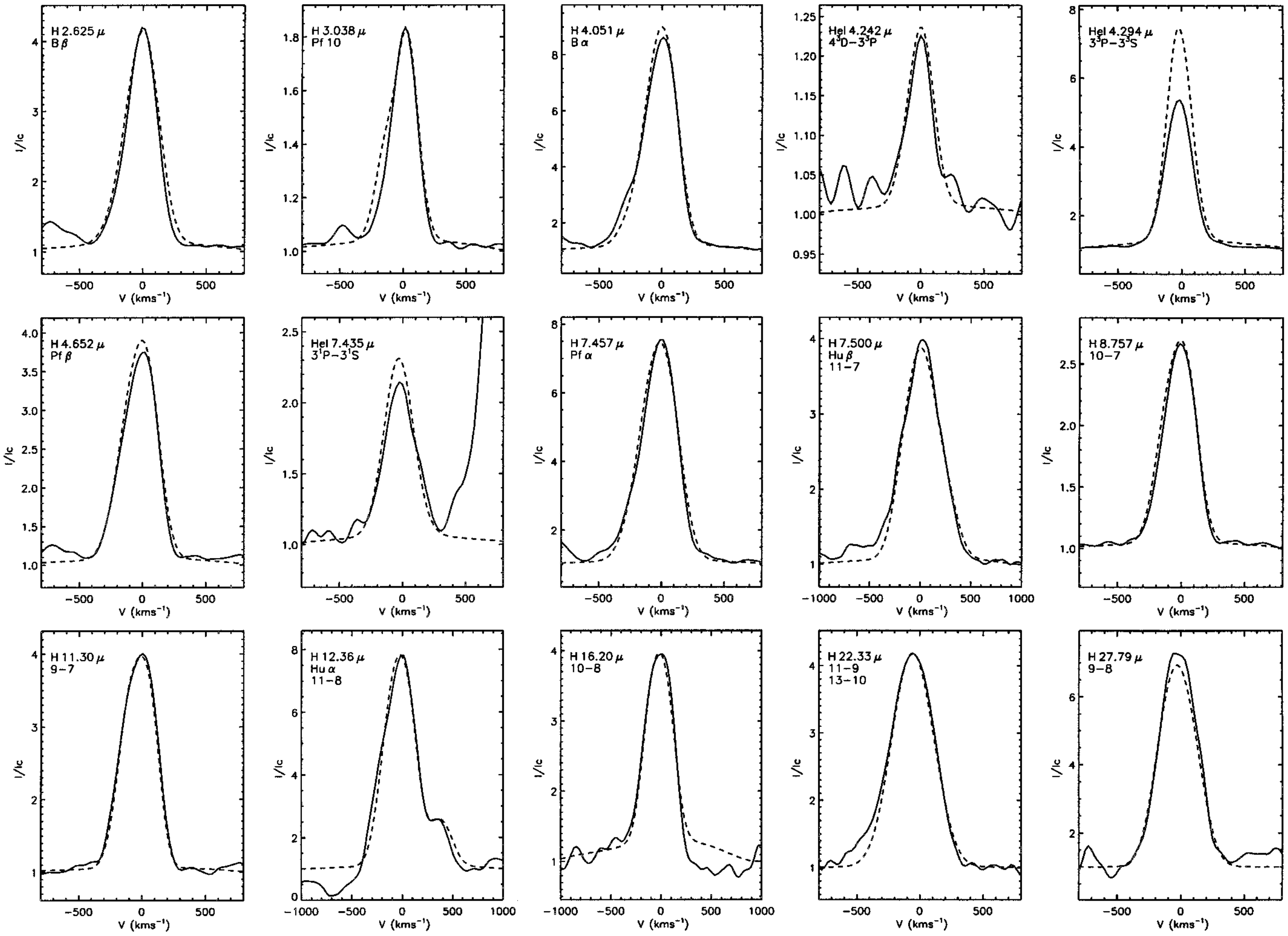

Fig. 1. Profiles fits (dashed) to the main ISO-SWS observed (solid) IR H and He I lines of P Cygni. Computed profiles have been degraded to the corresponding instrumental resolution. Each profile is labeled with the contributing component(s). Hydrogen profile fits include the corresponding He I components (see text).

Table 1. Derived stellar parameters for P Cygni from optical and infrared observations.

Model	R_*	L_*	T_{eff}	n_{He}/n_H	$\dot{M}$	v_∞	β	h_{eff}
	($R_\odot$)	($L_\odot$)	(10^4K)		($M_\odot$ yr^{-1})	(km s^{-1})		(R_*)
Optical	76	7.0×10^5	1.92	.29	3.2×10^{-5}	185	4.5	2.2×10^{-2}
ISO-SWS	76	5.6×10^5	1.81	.30	3.0×10^{-5}	185	2.5	2.2×10^{-2}

tive, non-LTE method presented by Hillier (1987, 1990) to solve the radiative transfer equation for the expanding atmospheres of early-type stars in spherical geometry, subject to the constraints of statistical and radiative equilibrium. Steady state is assumed, and the density structure is set by the mass-loss rate and the velocity field via the equation of continuity. The velocity law (Hillier 1989) is characterized by an isothermal effective scale height in the inner atmosphere, h_{eff}, and becomes a β law in the wind:

$$v(r) \approx v_o + (v_\infty - v_o)\{1 - R_*/r\}^\beta \quad (1)$$

where v_∞ is the terminal velocity and v_o regulates the transition zone between photosphere and wind. The atmosphere is considered to consist of hydrogen, helium and nitrogen (NII - NIII), where the latter is included to allow for its effect as a wind coolant (an abundance of $n_N/n_{He}=10^{-3}$ was assumed to account for mixing with CNO cycled matter, see below). The model atoms consisted of 15 H, 51 He I ($n \leq 11$) and 5 He II levels. The model is then prescribed by the stellar radius, R_*, the stellar luminosity, L_*, the mass-loss rate $\dot{M}$, the helium abundance, n_{He}/n_H and the velocity field, $v(r)$.

3.2. The fits to the observations

We started the analysis with the stellar parameters derived by Najarro (1995) based on a spectroscopic investigation of high resolution optical and near-IR spectra of P Cygni obtained by Stahl et al. (1993). We assumed a stellar radius of R_*=76 $R_\odot$ (Lamers et al. 1983). The value of the terminal velocity was held fixed at v_∞=185 km s^{-1}, which was derived from the high resolution optical profiles with R = 12000 by Stahl et al. (1993).

We then relaxed all other stellar parameters and proceeded to model the IR spectra of P Cyg in detail. The main observational constraints were set by the H and He I profiles measured with SWS, but consistency with the optical spectra was also required. Table 1 shows the model parameters which reproduce best the SWS lines together with those obtained by Najarro et al. (1996) from the optical spectroscopic investigation.

Notice that the stellar parameters obtained from both analyses agree fairly well. The main difference between the two models is the velocity field in the supersonic part of the wind. To match the optical high Paschen series lines we require a steep velocity field close to the photosphere, that switches to a flatter velocity law with β = 4.5 around v_o=80 km s^{-1}. However this velocity field results in much larger equivalent widths of the IR lines in the 2-7μm region than observed. In this spectral range the line formation regions of the main H and He I lines are located at $v(r) > 0.5v_\infty$, i.e., well beyond the transition zone between photosphere and wind, whereas the continuum is formed around v_o. Hence, if the velocity field is varied in the transition zone, the resulting changes in the equivalent widths will be primarily controlled by the variation of the continuum flux. Therefore, to reduce the computed equivalent widths in the 2-7μm region, a lower value of v_o (and hence a higher density and continuum flux) is required. This is achieved in our $ISO - SWS$ model where the transition between the steep photospheric velocity field and the wind regime occurs at about 30 km s^{-1} and the wind velocity law is steeper (β=2.5) than that derived from the optical spectrum. This model reproduces quite well both the optical and near-IR spectra of P Cygni, although it underestimates the absorption components of the high Paschen series members. This effect is related to the lack of metal line blocking in our models (Najarro, 1995). Due to the difference in the velocity and density structure of both models we derive a slightly lower effective temperature (ΔT_{eff}=1100 K) for the model based on the IR observations.

Figure 1 shows the excellent agreement of our calculations with the observations. Our model fits the profiles of the H and He I lines over the whole 2.5-28μm range. The model also accounts for the broad electron scattering wings of the strongest IR lines. The only discrepancy of our model with the observations is found for the He I 3^3S-3^3P line at 4.29μm. This is due to the lack of metal line blanketing in our models and its effects on the Balmer continuum (Najarro, 1995).

We conclude that the observed line spectrum can be fitted very well with a model with parameters given in Table 1.

4. The free-free emission

The IR energy distribution of P Cygni does not contain the signature of dust emission that is typically observed in other LBVs (Lamers, Morris et al. 1996). Therefore, the observed IR energy distribution has to be due entirely to the free-free and bound-free continuum of the extended atmosphere. To model this, we have scaled the continuum level of the $AOT1$ observations to that of the more accurate $AOT6$ scans. We also required that the different $AOT1$ scans match one another at their end points. This gives correction factors of 0.9 for Band 1, 0.93 for Band 2a, 0.95 for Band 2B and 1.0 for Band 2c. We estimate a photometric error of 10% in Band 1 and about 20% in Band 2. Figure 2 shows the resulting IR energy distribution from SWS, supplemented with other published measurements (Abbott et al. 1984, Waters and Wesselius, 1986).

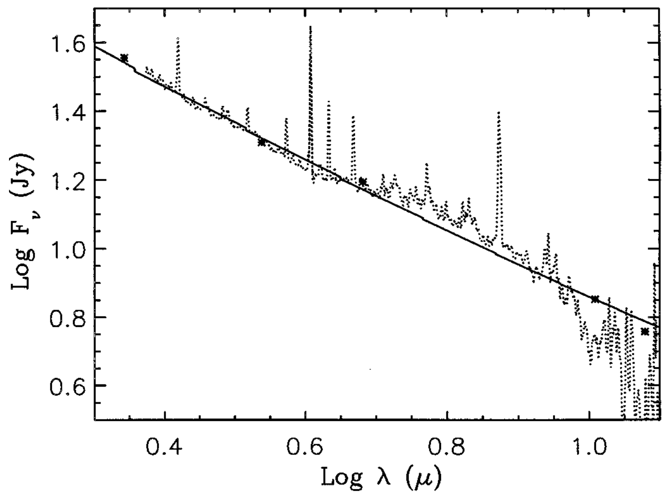

Fig. 2. SWS01 bands 1 and 2 observed spectral energy distribution of P Cygni compared with our model. The SWS flux beyond 9 μm is not reliable. Previous IR photometric observations are also shown (asterisks).

We found a good agreement between our model and the observations, if we adopt an extinction of $E(B-V)$ = 0.51 and the extinction law of Rieke et al. (1989). This is slightly smaller than the value of 0.63 derived by Lamers et al. (1983) on the basis of the UV energy distribution, but within the uncertainty of both determinations. Adopting the lower value, but keeping the radius constant, results in a distance of 1.71 kpc. This is within the accuracy of the cluster distance of 1.8 kpc (Lamers et al. 1983). Waters and Wesselius derived a slower velocity law than the one of our model, because they adopted a Rayleigh-Jeans energy distribution for the photosphere.

5. The emission lines of [Ne II] and [Ne III]

Numerous forbidden lines of [Si II], [Fe II], [Fe III], and [Ni II] are present in the spectrum of P Cyg. Figure 3 shows the lines of [Ne II] 12.81 μm measured with $AOT6$ and [Ne III] 15.55μm measured with $AOT1$ at lower resolution. The profiles shown here have not been corrected for instrumental broadening. The rectangular appearance of the [Ne II] line, and the reasonably close agreement between HWHM=170 km s^{-1}, derived after correcting for instrumental broadening, and v_∞=185 km s^{-1} indicates that the line is optically thin and formed almost entirely in the constant velocity region of the wind. The [Ne III] line is not resolved in the $AOT1$ scan. It is observed at 15.58 μm, but this may due to calibration errors in the early SWS spectra. There is no other possible candidate for this line than [NeIII] so we assume that the observed line is due to [NeIII].

The forbidden emission lines provide information about the CS envelope. We study the [Ne II] 12.81 μm and [Ne III] 15.55 μm lines using two-level model atoms, and assume that the

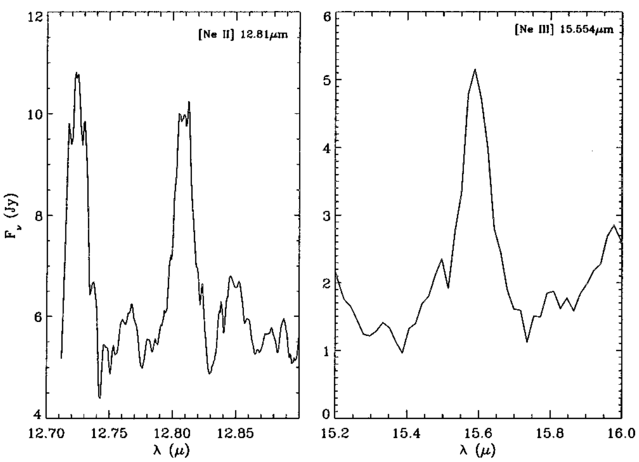

Fig. 3. Forbidden transtions of [Ne II] 12.81 μm measured with $AOT6$ ($left$) and [Ne III] 15.55 μm measured with $AOT1$ ($right$).

$14'' \times 27''$ detector area fully covers both the central source and nebula. We follow the method of Barlow et al. (1988).

The observed line flux at the earth of a fine-structure transition from upper level u to lower level l is given by

$$f = D^{-2} \int_0^\infty n_u A_{ul} h\nu r^2 dr, \quad (2)$$

where D is the distance of the star, n_u is the population density of the upper level in cm^{-3}, A_{ul} is probability for spontaneous transitions and ν is the line frequency. In statistical equilibrium, the total ion density is

$$n_i = n_u + n_l = n_u \left[1 + \frac{n_c + n_e}{n_e} \frac{g_l}{g_u} e^{h\nu/kT_e} \right], \quad (3)$$

where n_e is the electron density, g_u and g_l are the statistical weights of the upper and lower levels, and n_c is the critical density where the collisional and spontaneous de-excitation rates are equal. At $T_e \sim 10^4$ K the critical densities are 7×10^5 and 2×10^5 cm^{-3} for [Ne II] and [Ne III] respectively. The line emission will peak where $n_e \simeq n_c$, which corresponds to a radial distance of about 500 R_* for [Ne II]. The densities of eq. (3) can be expressed in terms of the mass loss rate. This allows the determination of the Ne^+ and Ne^{++} abundances from the flux of the two forbidden lines.

The line fluxes are $f([NeII])$ = 1.62×10^{-14} and $f([NeIII])$ = 5.0×10^{-14} W m^{-2}. Using the atomic parameters given by Barlow et al. (1988) and a He/H ratio of 0.3 we find ratios of Ne^+/H=1.3×10^{-4} and Ne^{++}/H=3.1×10^{-4} with an uncertainty of 30 % for Ne^+ and about a factor 2 for Ne^{++}. Adopting a cosmic abundance of Ne/H=8.3×10^{-5} we expect for the wind of P Cyg, which has a ratio of He/H=0.3, that Ne^+/H=1.4×10^{-4}. This agrees very well with the derived abundance of Ne^+, but it is a factor 0.3 lower than the sum of both observed ionization stages. The surface abundance of Ne in not expected to change during the evolution of a massive star untill the star enters the WC phase with very low H and N abundances. (Maeder and Meynet, 1993). So if the line at 15.58 μm is indeed due to [NeIII], the observed forbidden lines are too strong. This might be due to clumping in the CS envelope at a distance of 10^3 R$_*$, possibly due to ejections of slow and fast shells in the wind of P Cygni (Lamers et al. 1985) or to the interaction of the wind with ejecta from previous outbursts (Barlow et al. 1994). The allowed lines from which the mass loss rate was derived are formed much closer to the star at $r \simeq 10R_*$.

6. Summary and Conclusions

We have analysed the SWS spectrum of the LBV P Cygni. The IR emission lines and the IR continuum gives strong constraints on the density and velocity structure of the transition region between the photosphere and the wind. Using these data we derive an empirical model with the characteristics given in Table 1. The forbidden emission lines formed in the CS envelope provide information on the density and abundances. ¿From the lines of [Ne II] and [Ne III] we derive abundance ratios of Ne^+/H and Ne^{++}/H. The sum is about a factor three larger than expected from the cosmic abundance. This suggests that the lines are strengthened by clumping in the CS envelope at about 10^3 R$_*$.

In a forthcoming paper we will analyze the SWS-spectra of other luminous early type stars.

Acknowledgements. F. N. acknowledges a grant of the DARA under WE2- 50 OR 9413 6.

References

Abbott D.C., Telesco C.M., Wolf S.C. 1984, ApJ 279, 225
Barlow M.J., Roche P.F., Aitken D.K. 1988, MNRAS 232, 821
Barlow M.J., Drew J.E., Meaburn J., Massey R.M. 1994, MNRAS 268, L29
de Graauw Th., Haser L.N., Beintema D.A. et al. 1996, (this issue)
Hillier D.J., 1987, ApJ Suppl. 63, 947
Hillier D.J., 1989, ApJ 347, 392
Hillier D.J., 1990, A&A 231, 116
Humphreys R., Davidson K.D. 1994, PASP 106, 1025
Kessler M.F. et al. 1996, A&A Letters (this issue)
Lamers H.J.G.L.M. 1996 in *Astrophysical applications of stellar pulsation* eds. Stobie and Whitelock, ASP Conf Ser 83, p176
Lamers H.J.G.L.M., de Groot M.J.H. 1992, A&A 257, 153
Lamers H.J.G.L.M., de Groot M.J.H., Cassatella A. 1983, A&A 128, 299
Lamers H.J.G.L.M., Korevaar P. & Cassatella A. 1985, A&A 149, 29
Lamers H.J.G.L.M., Morris P.W. et al. 1996 (this issue)
Langer N., Hamann W.-R., Lennon M., Najarro F., Pauldrach A.W.A., Puls J, 1994, A&A, 290, 819
Maeder A., Meynet G. 1993, A&A 278, 406
Najarro F., 1995, PhD Thesis, University of Munich
Najarro F. et al. 1996 (in preparation)
Najarro F., Hillier D.J., Kudritzki et al. 1994, A&A 285, 573
Rieke G.H., Rieke M.J., Paul A.E. 1989, Ap.J 336, 752
Schaeidt S.G., Morris P.W., Vandenbussche B., et al. 1996 (this issue)
Stahl O., Mandel H., Wolf B., Gäng et al. 1993, A&AS 99, 167
Valentijn E.A., Feuchtgruber H., Kester D.J.M., et al. 1996 (this issue)
Waters L.B.F.M., Wesselius P.R. 1986, A&A 155, 104